SIMULATIONS OF BOOSTER INJECTION EFFICIENCY FOR THE APS-UPGRADE*

J. Calvey, M. Borland, K. Harkay, R. Lindberg, CY Yao, ANL, Argonne, IL 60439, USA

Abstract

The APS-Upgrade will require the injector chain to provide high single bunch charge for swap-out injection. One possible limiting factor to achieving this is an observed reduction of injection efficiency into the booster synchrotron at high charge. We have simulated booster injection using the particle tracking code elegant, including a model for the booster impedance and beam loading in the RF cavities. The simulations point to two possible causes for reduced efficiency: energy oscillations leading to losses at high dispersion locations, and a vertical beam size blowup caused by ions in the Particle Accumulator Ring. We also show that the efficiency is much higher in an alternate booster lattice with smaller vertical beta function and zero dispersion in the straight sections.

INTRODUCTION

The Advanced Photon Source (APS) booster synchrotron accelerates electron bunches from 375 MeV to 7 GeV before injection into the storage ring. In the present APS, the bunch charge typically ranges from 2 - 3 nC, which is sufficient for top-up operation. However, the APS-Upgrade will use swap-out injection [1,2], so the booster will need to provide the full charge in one shot, up to 16 nC for the 48 bunch "timing" mode. As a result, an R&D program was recently started to identify limitations to achieving reliable high-charge injection into the storage ring [3]. This paper will discuss recent progress in understanding and overcoming these limitations.

Booster Parameters

A list of booster parameters is given in Table 1. Parameters are given for two different lattices— the current operational lattice (which has 92 nm emittance [4]), and the original booster lattice (with 132 nm emittance [5]). One important difference between the two is that the 132-nm lattice has zero dispersion through the straight sections of the booster, which includes the RF cavities (Fig. 1). The 132-nm lattice has higher maximum dispersion, but a lower vertical beta function.

The booster is run off-momentum, i.e. the RF frequency does not match the booster circumference. This was a result of Decker distortion [6] in the storage ring, which shares an RF source with the booster. However, since running off-momentum results in a lower emittance (which is desirable for injection into the storage ring), we plan on retaining this feature for the upgrade.

* Work supported by the U.S. Department of Energy, Office of Science, Office of Basic Energy Sciences, under Contract No. DE-AC02-06CH11357.

Table 1: Booster Parameters

Parameter	**Value**	
Energy	0.375 - 7.0 GeV	
Ramp time	225 ms	
Circumference	368 m	
Revolution frequency	815 kHz	
RF Voltage	0.5 - 8.0 MV	
Parameter	**92 nm**	**132 nm**
Horizontal tune	13.75	11.75
Vertical tune	5.8	9.8
Avg. horiztonal beta function	7.87	7.93
Avg. vertical beta function	12.57	8.53
Momentum compaction	7.14×10^{-3}	9.71×10^{-3}
Energy offset	-0.085%	-0.06%

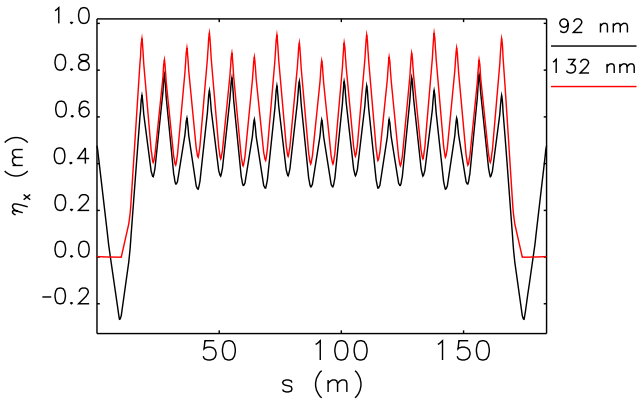

Figure 1: Horizontal dispersion for one half of the booster.

MEASUREMENTS

Initial attempts at improving the efficiency of the 92 nm lattice met with limited success. Fig. 2 (top) shows a typical example of stored current in the booster as a function of time. The 20 measurements shown were taken under nominally identical conditions, with 5-nC bunch charge. There is a significant loss of charge early in the ramp, which varies in magnitude shot-to-shot. Despite a great deal of effort (adjusting the RF voltage, chromaticity, tunes, correctors, etc.), we were not able to reliably extract more than 4 - 5 nC from the booster in this lattice. Interestingly, we found that increasing the RF voltage at injection actually made the initial losses worse.

The 132-nm lattice proved much easier to work with. As shown in Fig. 2 (bottom), the injection efficiency at 9 nC is ~90%, with only modest variation shot-to-shot.

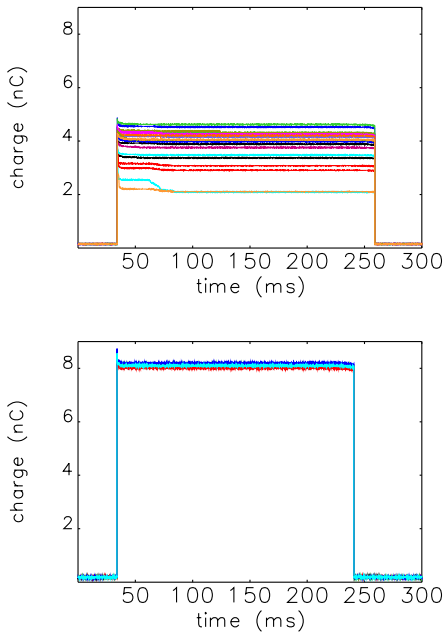

Figure 2: Bunch charge in the booster vs time: 92-nm lattice (top) and 132-nm lattice (bottom).

SIMULATIONS

To study these losses in detail, we used the particle tracking code `elegant` [7, 8]. A bunch, represented by 50,000 macroparticles, is tracked through a realistic booster lattice. The model includes element-by-element synchrotron radiation, the booster RF ramp, a detailed model of the transverse and longitudinal impedances (developed using the same techique applied to the storage ring [9]), and beam loading. To save computational time, only the first 3000 turns (~3.5 ms), where the majority of losses occur, are simulated.

Injected beam parameters

Whenever possible, injected beam paramters are taken from measurements. The transverse beam size as a function of charge was measured with a flag in the transfer line between the Particle Accumulator Ring (PAR) [10] and the booster. Of particluar interest is a blowup of the vertical beam size with charge, which we believe is caused by ions in the PAR [11]. The bunch length was measured with a streak camera in the PAR to be ~350 ps rms.

We also observe an rms energy mismatch between the injected beam and the booster, which we believe is caused by current variation in the dipole ramp. Based on measurements of the synchrotron oscillation amplitude at injection, we estimate this mismatch to be ±0.5% rms. In the simulation, this is represented by a fixed +0.5% mismatch in the beam energy.

Similarly, we observe an rms horizontal and vertical offset of the injected beam. The values for these offsets used in the simulation are taken from the measured amplitude of oscillations at the horizontal and vertical tune after injection.

Effect of energy mismatch

The simulations show that the injection efficiency is very sensitive to the energy mismatch described above. Fig. 3 plots the transmission vs time for a series of simulations with different values for this mismatch, for a 6-nC beam in the 92-nm lattice. The efficiency drops from 100% for no mismatch to less than 60% for a 1% mismatch. Fig. 4 overlays the energy oscillation of the beam centroid caused by the mismatch with the beam transmission; one can clearly see that the losses correspond with large negative energy deviation. The losses occur at locations with large dispersion, on the negative side of the horizontal aperture.

This effect also explains why increasing the RF voltage at injection reduced the measured efficiency, since the amplitude of energy oscillations for individual particles will increase with the voltage.

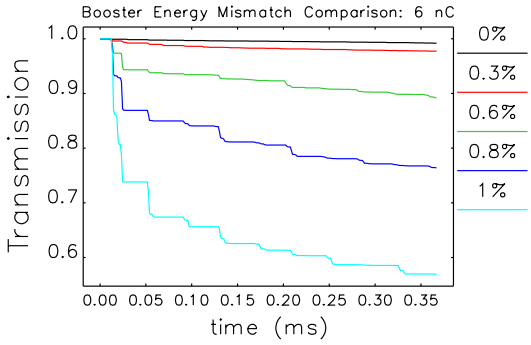

Figure 3: Transmission in the 92-nm lattice for different values of energy mismatch.

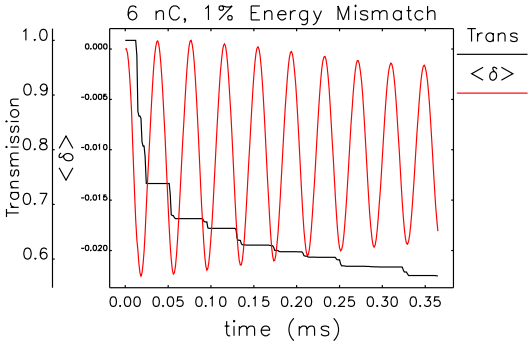

Figure 4: Transmission and centroid energy oscillations for a 1% mismatch.

Lattice comparison

Fig. 5 compares the simulated transmission vs time for both lattices, including all the effects described above. The simulation is consistent with the data: the 92-nm lattice shows a large charge-dependent drop in efficiency, with the majority of losses occuring very quickly. The 132-nm lattice has much higher efficiency up to 8 nC.

One important difference between the two lattices is that the 92-nm lattice has nonzero dispersion through the straight

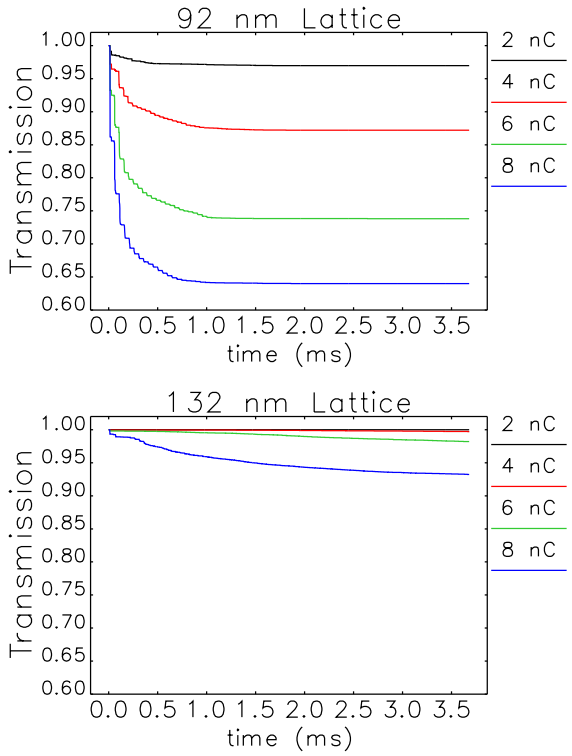

Figure 5: Transmission for different injected beam charge.

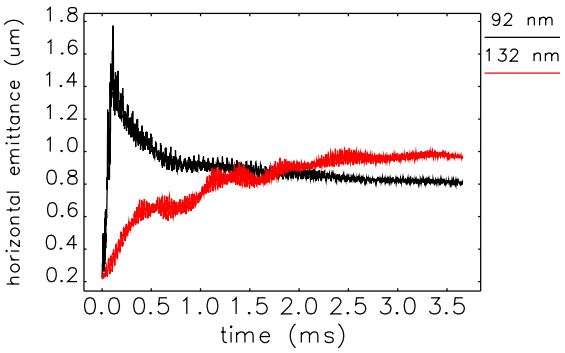

Figure 6: Simulated horizontal emittance: 8 nC.

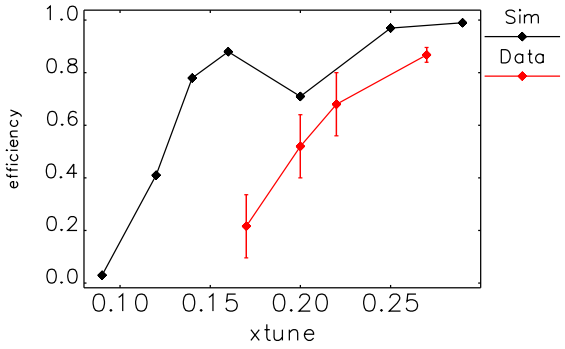

Figure 7: Transmission vs horizontal tune: 92-nm lattice, 2.5 nC. The error bars in the data represent the standard deviation of 20 successive measurements.

sections of the booster, which contain the RF cavities. The presence of dispersion in the RF cavities can lead to synchro-betatron coupling [12]. It has been shown [13, 14] that in the presence of collective effects, synchro-betatron coupling can lead to transverse emittance blowup, even away from resonance. As shown in Fig. 6, the simulation does predict a fast horizontal emittance blowup in the 92 nm lattice, which is not seen in the 132 nm lattice.

Further evidence for synchro-betatron coupling comes from measurements of the injection efficiency vs tune. Fig. 7 shows the efficiency (defined as the fraction of particles that survive 3000 turns) as a function of tune. The transmission drops suddenly as the horizontal tune approaches the synchrotron tune (which is ~0.025). This effect is seen in both measurements and simulations, though the decrease in efficiency is more severe in the measured data, possibly due to a drop in the horizontal tune after injection (caused by nonlinearities in the magnet ramps). The simulation was repeated for the 132-nm lattice and showed no dependence on tune.

High charge simulations

Simulations done for higher charge predict that the 132-nm lattice efficiency will begin to drop after ~10 nC. The losses occur on both the horizontal and vertical apertures, indicating that the beam size blowup could become important. Possible options for improving the efficiency at high charge include RF feedback or dynamic tuning of the RF cavities (to mitigate beam loading), shielding the booster bellows (to reduce the impedance), running the booster on-energy at injection (so the closed orbit passes through the center of the chamber), and mitigating the PAR ion effect through improved pumping or clearing electrodes.

CONCLUSIONS

Particle tracking simulations have been used to characterize losses shortly after injection into the APS booster synchrotron. The simulations indicate that the losses occur mainly on the horizontal aperture at high dispersion regions, due to energy oscillations caused by an rms mismatch between the injected beam energy and the booster. This effect may be worse in the 92-nm lattice due to synchro-betatron coupling caused by nonzero dispersion in the RF cavities.

REFERENCES

[1] R. Abela. *Proc. EPAC 92*, 486–488 (1992).

[2] L. Emery et al. *Proc.of PAC 2003*, 256–258 (2003).

[3] C. Y. Yao et al. *IPAC15*, 1828–1830 (2015).

[4] N. S. Sereno et al. *PAC03*, 247–249 (2003).

[5] S. V. Milton. *PAC95*, 594–596 (1996).

[6] G. Decker et al. *Phys Rev ST Accel Beams*, 2 (11):112801 (1999).

[7] M. Borland. ANL/APS LS-287, Advanced Photon Source (2000).

[8] Y. Wang et al. *Proc. of PAC 2007*, 3444–3446 (2007).

[9] R. R. Lindberg et al. *Proc. IPAC 2015*. TUPJE078.

[10] M. Borland. *PAC 1995*, 287 (1996).

[11] J. Calvey et al. *THPOA14, these proceedings*.

[12] A. Piwinski. DESY 93-189, DESY (1993).

[13] J. Hagel et al. CERN/LEP-TH/88-57, CERN (1988).

[14] K. Nakajima et al. *Part Accel*, 27:77 (1990).